Extremophiles (2003) 7:9–16
DOI 10.1007/s00792-002-0290-7

ORIGINAL PAPER

**Eva Nordberg Karlsson · Susan J. Crennell
Catherine Higgins · Salina Nawaz · Louisa Yeoh
David W. Hough · Michael J. Danson**

Citrate synthase from *Thermus aquaticus*: a thermostable bacterial enzyme with a five-membered inter-subunit ionic network

Received: 4 March 2002 / Accepted: 9 July 2002 / Published online: 7 September 2002

Abstract A bacterial thermostable citrate synthase has been analyzed to investigate the structural basis of its thermostability, and to compare such features with those previously identified in archaeal citrate synthases. The gene encoding the citrate synthase from *Thermus aquaticus* was identified from a gene library by screening with a PCR fragment amplified from genomic DNA using a primer based on the determined N-terminal amino acid sequence and a citrate synthase consensus primer. Apart from high sequence similarities with citrate synthase sequences within the *Thermus*/*Deinococcus* group, the analyzed enzyme has highest similarities with the enzyme from the hyperthermophilic Archaeon *Pyrococcus furiosus*. The recombinant enzyme is a dimer with high specific activity. Compared to its thermoactivity (T_{opt} at 80°C), the thermal stability of the enzyme is high, as judged from its T_m (101°C), and from irreversible thermal inactivation assays. Molecular modeling of the structure revealed an inter-subunit ion-pair network, comparable in size to the network found in the citrate synthase from *P. furiosus*; these networks are discussed in relation to the high thermal stability of these bacterial and archaeal enzymes.

Keywords Citrate synthase · Protein thermostability · Thermophile · *Thermus*

Communicated by G. Antranikian

S.J. Crennell · C. Higgins · S. Nawaz · L. Yeoh
D.W. Hough · M.J. Danson (✉)
Centre for Extremophile Research,
Department of Biology and Biochemistry,
University of Bath,
Bath BA2 7AY, UK
E-mail: m.j.danson@bath.ac.uk
Tel.: +44-1225-386509
Fax: +44-1225-386779

E. Nordberg Karlsson
Department of Biotechnology,
Center for Chemistry and Chemical Engineering,
Lund University, Lund, Sweden

Introduction

Citrate synthase (EC 4.1.3.7) catalyzes the condensation of oxaloacetate and acetyl-CoA to form citrate and CoA. The enzymes from Archaea, Gram-positive Bacteria, and Eukarya are dimers of identical subunits (Danson and Hough 1998), whereas those from Gram-negative bacteria are generally homo-hexamers (Nguyen et al. 2001). In all cases, the active sites lie between subunits, and therefore the dimer can be considered as the basic catalytic unit in both types of citrate synthase.

We have previously characterized and determined the atomic structures of several dimeric citrate synthases from a range of organisms whose optimal growth temperatures span the biological range of temperatures (10° to 100°C) (Bell 1999; Russell et al. 1994, 1997, 1998), these being in addition to the already determined structure of pig and chicken enzymes (Remington et al. 1982). Detailed comparisons have helped to identify structural trends that appear to be associated with the increasing thermostability of this series of enzymes (Danson and Hough 1998). These include increased compactness as a consequence of shorter surface loops, reduction in internal cavities, increased internal packing through isoleucine clusters, and greater complementarity at the subunit interface. Furthermore, consistent with observations on a number of other hyperthermophilic enzymes (Karshikoff and Ladenstein 2001), the citrate synthase from *Pyrococcus furiosus* (optimal growth at 100°C) has two 5-amino acid inter-subunit ionic networks that site-directed mutagenesis studies indicate make important contributions to the protein's hyperthermostability (Arnott et al. 2000). Ionic bonds may also stabilize the loops of this enzyme, as might interactions between the C-terminal arm of each polypeptide with its partner subunit within the dimer (Russell et al. 1997).

All the investigated citrate synthases from thermophilic and hyperthermophilic organisms are so far of archaeal origin: *Pyrococcus furiosus* (Muir et al. 1995;

Russell et al. 1997), *Sulfolobus solfataricus* (Bell 1999; Connaris et al. 1998), and *Thermoplasma acidophilum* (Sutherland et al. 1990, 1991; Russell et al. 1994). Therefore, it is of interest to compare these archaeal enzyme structures with a bacterial thermostable citrate synthase, in order to reveal whether the same stabilizing principles are used in the enzymes of thermophilic organisms other than the Archaea. For this reason, we chose to investigate the citrate synthase from the thermophilic bacterium *Thermus aquaticus*. Staining of the cell walls of bacteria belonging to the genus *Thermus* indicates that they are Gram-negative organisms, but they have many other features that appear more consistent with Gram-positive bacteria (Williams and Sharp 1995). Moreover, the citrate synthase found in *T. aquaticus* is a dimeric protein, which is more consistent with the Gram-positive bacteria (Weitzman 1978), and which should then allow a more direct comparison with the archaeal homologs.

In this paper we describe the cloning, sequencing, and heterologous expression of the gene encoding the *T. aquaticus* citrate synthase, and an investigation of the thermostability of the recombinant enzyme. Based on its relatively high sequence identity with the hyperthermophilic citrate synthase from *P. furiosus*, we have also modeled the structure of the *T. aquaticus* enzyme, and provide evidence that it possesses an inter-subunit ionic network comparable with that found in the archaeal homolog. The findings are discussed in the context of how Nature has solved the structural basis of protein thermostability (for recent reviews, see Sterner and Liebl 2001; Vielle and Zeikus 2001).

Materials and methods

Bacterial strains and vectors

Thermus aquaticus (strain YT1) cells were a kind gift from Dr. N. Raven, Centre for Applied Microbiology and Research, Porton Down, Salisbury, UK. *Escherichia coli* strain XL1-blue with the vector pUC18, and strain JM109 with the vector pGEM-T (Promega), were used for cloning of PCR-amplified consensus fragments. A genomic library was constructed in λ EMBL3 using *E. coli* XL1-blue MRA host cells. For expression, the vector pREC7/*Nde*I (provided by Dr. L.C. Kurz, Washington University School of Medicine, St Louis, MO, USA) was used in the citrate synthase-negative *E. coli* strain W620 (*gltA6, relA1, supE44, thi-1, pyrD36, galK30, rpsL129, Smr*).

Purification of native and recombinant citrate synthase

T. aquaticus cells, or *E. coli* cells expressing the recombinant *T. aquaticus* citrate synthase, were lysed using a single-shot cell disrupter (Constant Systems Ltd, Warwick, UK) in 20 mM Tris-HCl, pH 8.0, 2 mM EDTA, followed by centrifugation at 20,000 *g* for 20 min. The cell extract from *E. coli* cells was heat treated at 65°C for 15 min, and again centrifuged (20,000 *g*, 30 min). Citrate synthase from the *T. aquaticus* cell extract and the heat-treated *E. coli* extract was purified using a Matrex Gel Red A (Amicon, UK) column equilibrated with the above Tris/EDTA buffer. Unbound protein was removed by washing in 5 volumes of the same buffer, and citrate synthase was then biospecifically eluted by 1 mM CoA and 5 mM oxaloacetate in the Tris/EDTA buffer (James et al. 1994).

Gel filtration

Pooled fractions containing citrate synthase were applied to a Superdex 200 gel filtration column (Amersham Pharmacia Biotech UK Ltd, Bucks, UK), pre-equilibrated with 20 mM Tris-HCl buffer, pH 8.0, containing 2 mM EDTA, 25 mM NaCl and 0.1 M KCl. The column was calibrated with the following molecular mass markers: bovine thyroglobulin ($M_r = 663{,}000$), horse spleen apoferritin (443,000), sweet potato β-amylase (200,000), yeast alcohol dehydrogenase (150,000), bovine serum albumin (66,000), bovine carbonic anhydrase (29,000) and horse cytochrome *c* (12,400). Elution volumes (V_e) were expressed relative to that of Dextran Blue (V_o) and the data (M_r versus V_e/V_o) were fitted to an exponential curve.

N-terminal sequence analysis

Purified native citrate synthase from *T. aquaticus* was electrophoresed through a 10% (w/v) SDS-polyacrylamide gel according to Laemmli (1970), and subsequently transferred to a polyvinyl difluoride (PVDF) membrane (Millipore, Bedford, MA, USA) by semi-dry electroblotting using the Multiphor II NovaBlot Unit (Amersham Pharmacia Biotech). The membrane was stained with Coomassie Brilliant Blue and excised protein bands were sequenced using a 470A Applied Biosystems Gas Phase Sequencer coupled to a phenylhydantoin analyzer.

PCR-amplification of part of the *Thermus aquaticus* citrate synthase gene

Taking into account codon usage in *T. aquaticus*, a forward degenerate primer (*A*) was designed [5′-3′ ATG GA(G,A) GT(G,C) GC(C,G) AGG, GG(G,C) CT(G,C) GA] using the first eight amino acids of the determined N-terminal sequence [MEVARGLEGVLFTETRMCFIDGEA GRLY]. A degenerate consensus reverse primer (*B*) was also designed [3′-5′ TTG CA(C,A) CT(G,A) AA(G,A) AT(G,A) AG(G,C) CC(T,G)] from the alignment of the amino acid sequences of six Gram-negative bacterial citrate synthases (from *Acinetobacter anitratum*, *Pseudomonas aeruginosa*, *E. coli*, *Coxiella burnetti*, *Acetobacter aceti*, and *Rickettsia prowazekki*). The sequence corresponds to the conserved residues NVDFYSG, and again the codon usage of *T. aquaticus* was considered in the primer design.

The standard PCR technique was used to generate a 938-bp fragment using genomic DNA as template, prepared according to Sambrook et al. (1989). Amplification was carried out in a 100-µl reaction with 250 ng template DNA added to 200 µM dNTPs, 1 mM $MgCl_2$ and 0.1 µM of each primer (*A* and *B*). After a 96°C hotstart for 5 min, 1.25 U *Taq*-polymerase was added (1 min hold at 85°C) and amplification was allowed to proceed for 30 cycles (96°C for 1.5 min, 45°C for 1 min, 72°C for 2 min), with a final extension at 72°C for 7 min.

Construction and screening of a *Thermus aquaticus* genomic library

Genomic DNA was partially digested with *Sau*3AI, purified by extraction with phenol:chloroform:isoamyl alcohol (25:24:1), and precipitated with absolute alcohol. The resuspended DNA was separated by density gradient centrifugation using 5–25% (w/v) NaCl. Fractions containing 15-kb fragments were ligated to λ EMBL-3 phage arms (Gigapack III Gold, Stratagene) pre-digested with *Bam*HI, and packaged into phage particles according to the manufacturer's instructions.

Plaques formed after incubation with the host cells (*E. coli* XL1-blue MRA) were transferred to nylon membranes (Hybond

N^+), denatured, neutralized and baked as described by Sambrook et al. (1989). The cloned and sequenced 938-bp PCR-fragment (described above) was used as a probe. The fragment was first excised from plasmid pGEM-T using *Aat*II and *Not*I, and random-primed DNA labeling was performed using [α-^{32}P]-dCTP (Boehringer Mannheim, Germany). Membranes were hybridized overnight at 52°C, washed twice at 52°C (1×SSC, 0.5% SDS for 20 min, followed by 0.5×SSC, 0.5% SDS for 30 min), and then exposed to X-ray film overnight at –70°C. Positive plaques were picked and re-screened as described above. DNA from positive plaques was extracted using the λ DNA Maxi preparation kit (Qiagen, UK) and sequenced using the dideoxynucleotide chain termination method (Sanger et al. 1977) on an Applied Biosystems 377 automated sequencer.

PCR amplification and expression of the complete citrate synthase gene

Based on the determined sequence of the entire citrate synthase gene and its flanking regions, two primers were designed (C and D) to effect the cloning of the gene into the expression-vector pREC7/*Nde*I. The forward primer (*C*) [*Nde*I-site underlined: 5′-CATGATAGCATATGGAAGTGGCACGGGG-3′], and the reverse primer (*D*) [*Kpn*I-site underlined: 5′-CATGGTACCTCAGCCCCTGGCCTCCAG-3′] were used at concentrations of 100 μM each in a reaction volume of 50 μl containing purified genomic DNA (1 μg), 0.2 mM dNTPs, 1 mM $MgCl_2$. After a 96°C hot-start for 5 min, 2.5 U *Taq*-polymerase was added, and amplification was allowed to proceed for 30 cycles (96°C for 1.5 min, 60°C for 1 min, 72°C for 2 min), with a final extension at 72°C for 7 min. After electrophoresis on 0.5% agarose gels and purification using the Qiaex II gel extraction kit, the PCR-amplified fragment was ligated into the pREC7/*Nde*I vector and the gene sequence was checked. After transformation into the citrate synthase-negative strain *E. coli* W620, cells were grown in Terrific Broth at 37°C to logarithmic phase, induced by nalidixic acid (50 μg/ml) and further incubated for 20 h before harvesting.

Structural modeling

The primary sequence of the *T. aquaticus* citrate synthase was homology modeled to the 1.9Å crystal structure of the *P. furiosus* enzyme using the program O (version 6.2.1, Jones et al. 1991). Equivalent residues were identified from a sequence alignment constructed using the program GAP (Wisconsin Package version 8.0; GCG, Madison, WI, USA) with all deletions and insertions moved, if necessary, to be outside the secondary-structural regions. Amino acid side chains with unknown coordinates were built with ideal geometries using the O rotamer library. The dimer was created from a modeled monomer by rotation about the two-fold axis. The main-chain geometry was plotted on a Ramachandran plot as implemented in PROCHECK (Collaborative Computational Project 1994) and amino acid environments were examined using the three-dimensional profile method (Luthy et al. 1992; at http://www.doe-mbi.ucla.edu/services/verify3D.html); both were altered where necessary.

Citrate synthase assays and kinetic analysis

Citrate synthase activity was assayed as previously described (Srere et al. 1963). The assay mixture (1 ml) contained 0.2 mM oxaloacetate, 0.2 mM acetyl-CoA and 0.1 mM 5,5′-dithiobis-(2-nitrobenzoic acid) in a buffer composed of either 20 mM Tris-HCl, pH 8, 2 mM EDTA, 0.1 M KCl, or 50 mM sodium phosphate buffer, pH 7, 1 mM EDTA, 0.1 M KCl. The assay temperature was 55°C unless stated otherwise. For determination of kinetic parameters, the concentration of one substrate was varied whilst the second was kept at a saturating concentration (20× K_m). K_m and V_{max} values were calculated from these data by the direct linear plot of Eisenthal and Cornish-Bowden (1974) using the Enzpack3 computer software (Biosoft, Cambridge, UK).

The dependence of catalytic activity on temperature was studied by assaying the initial citrate synthase activity in the temperature range 30°–95°C, using 50 mM sodium phosphate buffer, pH 7, 2 mM EDTA, 0.1 M KCl. The dpK_a/dT of the buffer was used to ensure that a value of pH 7 was attained across the temperature range used.

Thermal inactivation and denaturation

Thermal inactivation studies were carried out by incubating citrate synthase (0.1 mg/ml) in 50 mM phosphate buffer, pH 7.0, 2 mM EDTA, 0.1 M KCl, at a given temperature. Aliquots were removed at known intervals and rapidly cooled in ice. Remaining enzyme activity was measured at 55°C in the same buffer (after an incubation period on ice for at least 1 h) under the assay conditions described above.

The unfolding transition temperature (T_m) of the purified recombinant citrate synthase (0.1 mg/ml in 50 mM phosphate buffer, pH 7.0, 2 mM EDTA, 0.1 M KCl) was measured by differential scanning calorimetry (DSC) using a VP-DSC (MicroCal, USA) (Plotnikov et al. 1997) at a scan-rate of 60°C/h in the temperature range 20°–130°C.

Total protein estimation

Total protein concentrations were determined by the method of Bradford (1974) using bovine serum albumin as the standard protein.

Nucleotide sequence accession number

The sequence reported in this study has been deposited in the EMBL database under the accession number AJ417978.

Results

Cloning and sequencing of the *T. aquaticus* citrate synthase

Amplification of *T. aquaticus* gDNA, using a forward primer based on the determined N-terminal amino acid sequence of the native citrate synthase and a reverse degenerate consensus primer, gave rise to a 938-bp gene-specific fragment whose sequence showed a high identity to known bacterial citrate synthase sequences. A *T. aquaticus* genomic library was created using the λ EMBL 3 phage system, and screened using the 938-bp gene fragment. After repeated screening of positive plaques, one clone was selected and both strands were sequenced with gene specific primers based on the already known partial sequence. The translated amino acid sequence is given in Fig. 1, the N-terminal sequence exactly matching the 28-amino acid sequence determined from the native citrate synthase purified from *T. aquaticus* cells.

The citrate synthase gene (1,134-bp) encodes a protein of 377 amino acids (M_r = 42,200). It is preceded by a ribosomal binding site (5′-GGAGG-3′) located 10 bp upstream of the start codon (ATG). The citrate synthase described here is 91% identical to a deposited putative citrate synthase sequence from the genome sequence of *T. aquaticus* ssp *thermophilus* (accession number

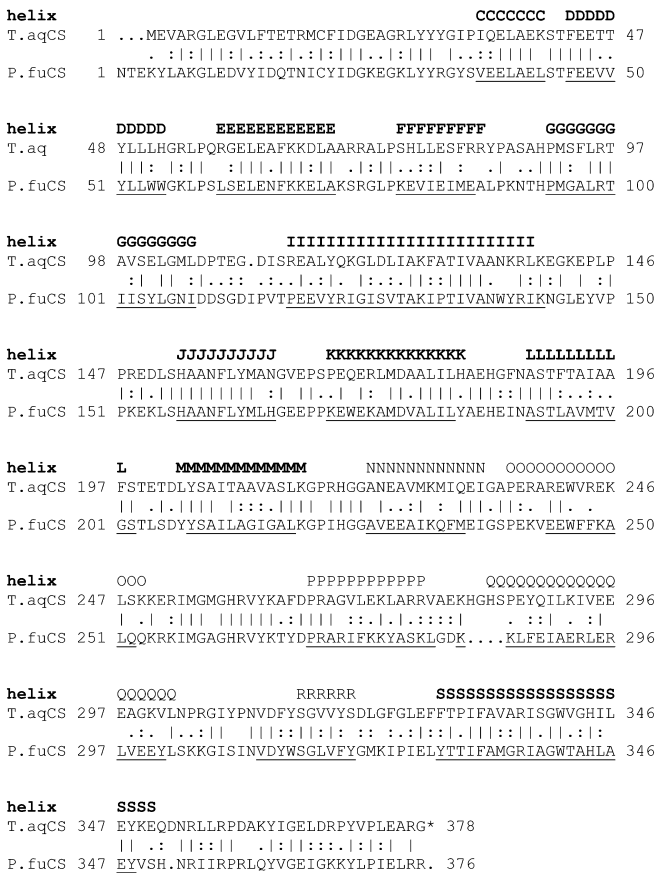

Fig. 1 Alignment of the amino acid sequences of citrate synthases from *Thermus aquaticus* (*T.aqCS*) and *Pyrococcus furiosus* (*P.fuCS*). Amino acid sequence identities are shown by a v*ertical line* and conservative replacements by a *double dot*. The modeled alpha helices [numbered according to pig citrate synthase (Remington et al. 1982)] of the *T. aquaticus* enzyme are *shown above* the amino acid sequence. The helices of the large domain are indicated in *bold capital letters*, and the helices of the small domain in *normal capital letters*. The positions of the equivalent helices in *P.fuCS*, as determined from the crystal structure, are shown by *underlining the sequence*

AB040146). Apart from this very closely related citrate synthase, it is 56% identical to a citrate synthase sequence from *Deinococcus radiodurans* R1, also in the *Thermus*/*Deinococcus*-group (White et al. 1999). More remarkably, it shows high sequence identity (47%) with the archaeal *P. furiosus* citrate synthase, whose catalytic properties and 3D-structure with bound ligands have been determined (Muir et al. 1995; Russell et al. 1997). As noted for the archaeal citrate synthases, and those from Gram-positive bacteria, the *T. aquaticus* citrate synthase is approximately 40 residues shorter at the N-terminus than the citrate synthases described from eukaryotes and Gram-negative bacteria (Muir et al. 1995).

Purification and characterization of native and recombinant citrate synthase from *T. aquaticus*

Affinity chromatography on Matrex Gel Red A was used to effect the purification of both native and recombinant citrate synthases of *T. aquaticus*. In the case of the native enzyme, this single step gave a purity of approximately 70%, as judged by SDS-PAGE, and a specific activity of 90 μmol/min/mg enzyme. This purification was sufficient to enable the N-terminal sequencing of the enzyme for the eventual cloning, sequencing, and heterologous expression of the citrate synthase gene. With the recombinant enzyme, homogeneity was achieved when the affinity chromatography step was preceded by a heat treatment of the cell extract, to remove host cell proteins (Table 1). The specific activity of 125 μmol/min/mg is consistent with the recombinant having a very similar activity to the native enzyme, allowing for their different purities. With respect to their kinetic parameters [at an assay temperature of 55°C, native enzyme: K_m (acetyl-CoA = 25 (± 3) μM and K_m (oxaloacetate) = 33 (± 5) μM; recombinant enzyme: K_m (acetyl-CoA) = 11 (± 2) μM, K_m (oxaloacetate) = 10 (± 2) μM], it does appear that the recombinant citrate synthase does have a slightly lower *K*m values than the native enzyme.

Neither recombinant nor native enzyme accept *n*-propionyl-CoA as an alternative substrate; that is, they have no detectable 2-methylcitrate synthase activity. In this aspect, the *T. aquaticus* citrate synthase differs from the dimeric citrate synthases of the thermophilic Archaea, *P. furiosus* and *T. acidophilum*, and the cold-active citrate synthase from the Antarctic bacterium, *Arthrobacter* strain DS2–3R, which all exhibit 2-methylcitrate synthase activities (Gerike et al. 1998).

The dimeric nature of the *T. aquaticus* citrate synthase (Weitzman 1978) was confirmed with the recombinant enzyme by SDS-PAGE (M_r = 43,000) and gel filtration (M_r = 100,000).

The temperature optimum of catalytic activity for both the native and recombinant enzymes, measured over a time period of 1 min, was 80°C, at which temperature the specific activity was 300 μmol/min/mg. Interestingly, at 85°C the half-life of the enzyme was 70 min and the pseudo-first-order rate constant for irreversible thermal inactivation was 0.009 (± 0.002) min^{-1}. Thermal unfolding using DSC showed the enzyme to have a T_m of 101°C. As expected, on these criteria, the thermostability and thermoactivity of the citrate synthase from *T. aquaticus* (optimum growth temperature of 70°C) is mid-way between the enzyme of *T. acidophilum* (55°C) and *P. furiosus* (100°C).

Molecular modeling

On account of their high sequence identity, we were able to use the structure of the *P. furiosus* citrate synthase as a template for modeling the *T. aquaticus* enzyme structure. A 3D-1D-profile plot of the modeled monomer, showing all residues in acceptable environments, supported the structural validity of the generated model. As in all citrate synthases determined to date, the subunits of the modeled *Thermus* enzyme have a high helical

Table 1 Purification of the recombinant citrate synthase from *Thermus aquaticus*

Purification step	Volume (ml)	Total activity (μmol/min)	Total protein (mg)	Specific activity (μmol/min/mg)	Yield (%)	Purification
Cell extract	5	375	31	12	100	1.0
Heat treated extract	5	375	14	27	100	2.2
Matrex Gel Red A	22	214	1.7	126	57	10.3

content and each comprises a large (helices C-G, I-M, and S) and a small (helices N-R) domain. The helix numbering system is that of the pig citrate synthase (Remington et al. 1982), and thus it can be seen that, like the thermophilic archaeal citrate synthases (Bell 1999; Connaris et al. 1998; Russell et al. 1994, 1997), the enzyme from *T. aquaticus* lacks helices A, B, H and T.

Keeping in mind the limits of a modeled structure, three aspects of the *T. aquaticus* citrate synthase structure can be discussed and compared with the already-determined structures.

Active site

The active sites of all dimeric citrate synthases lie in a cleft between the two subunits. Putative catalytic and substrate binding residues of the *T. aquaticus* citrate synthase were identified by structural comparison of the model with the structure of the *P. furiosus* citrate synthase (Russell et al. 1997). In the *Thermus* enzyme, the three principal catalytic residues (His219, His258 and Asp312), and the six citrate binding residues (His184, His219, His258, Arg267, Arg337, Arg356′, the prime indicating that the residue comes from the second monomer) are structurally conserved. Primary sequence and structural conservation is also high around the residues involved in CoA binding. In the *Pyrococcus* enzyme two ligands (Lys254, Lys305) interact with the 3′-phosphate of CoA, and in the *Thermus* citrate synthase these are Lys250 and Arg305. In addition, the *Thermus* enzyme has five putative ligands in the vicinity of the α- and β-phosphates of CoA, compared with four in *Pyrococcus*. Arg218 is the extra ligand in the *Thermus* enzyme (Fig. 2), and is the only arginine present in this position in the primary sequence in an alignment of 60 citrate synthase sequences. Since this residue immediately precedes a conserved catalytic residue (His219, as shown in Fig. 2) and is within a ten-amino-acid region of high homology among citrate synthases, it is highly probable that Arg218 lies in the position shown and thus is a CoA binding residue. The other four putative ligands (Arg252, Arg259, Lys262, Arg353′) are conserved between *Thermus* and *Pyrococcus* citrate synthases, and involve both monomers in the interaction.

Subunit interface

In all citrate synthases whose structures have been determined, the subunit interface is formed by an eight

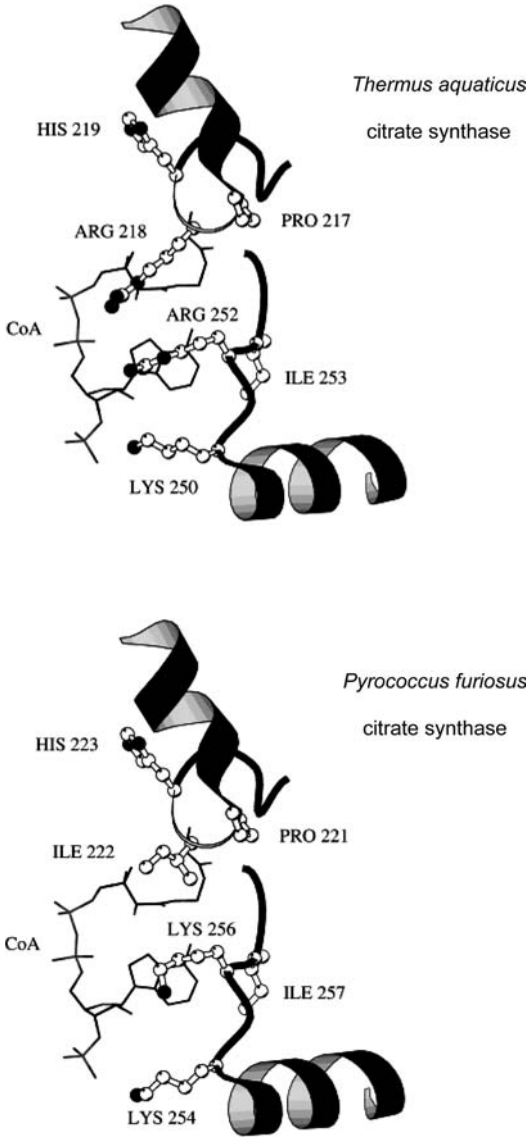

Fig. 2 The unique CoA binding residue (Arg218) of *T. aquaticus* citrate synthase is shown together with its surrounding residues. The homologous structure of the *P. furiosus* enzyme is shown for comparison. The amino acid side chains are shown in *ball and stick* representation, and CoA is shown by *thin lines*

α-helical sandwich, comprising four anti-parallel pairs of helices (F, G, M and L). In the *Pyrococcus* enzyme, two inter-subunit ion-pair networks, each involving five amino acid residues from helices G and M, have been proposed to contribute significantly to the protein's hyperthermostability (Russell et al. 1997; Arnott et al.

2000). Four of the five residues involved are conserved in the *T. aquaticus* citrate synthase, whereas the fifth amino acid (Asp113 in the *Pyrococcus* enzyme), crucial to the interactions of the network, is absent in the *Thermus* enzyme. However, Glu109, accompanied by an altered G-I loop conformation due to a single residue deletion, may partially restore the network in the *Thermus* citrate synthase (Fig. 3).

The six-membered isoleucine cluster that is found at the subunit interface of the *Pyrococcus* citrate synthase is not present in the *T. aquaticus* enzyme. The total number of isoleucine residues (19) is also lower than the number found in any of the thermostable archaeal citrate synthases (34 in *P. furiosus*, 31 in *T. acidophilum*, and 27 in *S. solfataricus*).

Loops

The lengths of the inter-helical loop regions in the *T. aquaticus* enzyme appear to be rather similar to those found in the citrate synthases from the thermophilic Archaea, and are thus shorter than those in the mesophilic enzymes. This trend towards shorter or absent loops in thermophilic proteins has been suggested as a general strategy for thermostabilization (Thompson and Eisenberg 1999). In the structural comparisons of citrate synthases we have also noticed that the thermostable enzymes have extensive ionic interactions that cross-link loop regions. Interestingly, many of the charged amino acids in the loops of the *P. furiosus* citrate synthase are conserved in the *T. aquaticus* enzyme, although from a structural model it is not possible to state definitively that they form stabilizing electrostatic interactions. Also of possible significance is the observation that of the eight loop prolines found in *P. furiosus* citrate synthase, but which are absent from the cold-active enzyme (Russell et al. 1998), five are conserved in the loops of the *Thermus* enzyme.

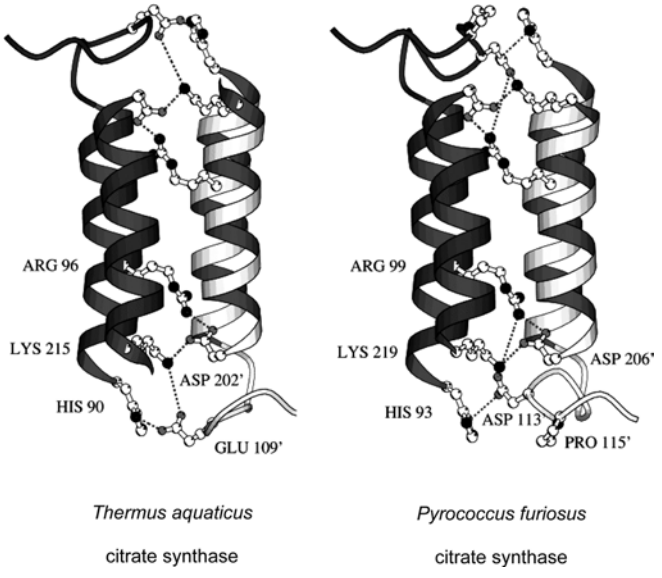

Fig. 3 Comparison of the inter-subunit ion-pair network in the *T. aquaticus* and *P. furiosus* citrate synthases. Helices G (*Thermus* citrate synthase: amino acids 91–105) and M (204–216) are shown in *dark and light shadings* for the two subunits of the dimer, for which the amino acid residues of the ionic networks are labeled *without and with primes*, respectively. Four of the five *Pyrococcus* residues in the network are conserved in the *Thermus* enzyme. The fifth residue is a conservative replacement (Glu for Asp); its position has shifted, but it is still located in the loop after helix G

Discussion

Archaeal citrate synthases are homo-dimeric enzymes, the polypeptides of which are approximately 40–50 amino acids shorter than those comprising the dimeric eukaryotic citrate synthases. In selecting a bacterial citrate synthase for comparison with the well studied, thermophilic archaeal enzymes, that from *T. aquaticus* was chosen as it had already been shown to be a thermostable, dimeric protein (Weitzman 1978). Moreover, in this paper, we show that its constituent polypeptides are of the shorter length, providing an additional reason for it being a valid choice with which to compare the archaeal homologs.

We chose to purify the native citrate synthase from cells of *T. aquaticus* for two reasons. First, organisms are known which have more than one 'citrate synthase' gene. In *E. coli*, for example, we have shown that one gene encodes the hexameric citrate synthase while the other produces a dimeric enzyme that is principally a 2-methylcitrate synthase (uses propionyl-CoA and oxaloacetate), although it also has minor activity with acetyl-CoA. The predominant activity cannot be deduced from sequence alone, and therefore we needed to ensure that the gene to be cloned from *T. aquaticus* coded for a true citrate synthase. That is, an N-terminal amino acid sequence from the purified enzyme was obtained from which a gene-specific oligonucleotide probe could be designed. Secondly, native enzyme is required with which to compare the recombinant version to ensure that the latter has folded correctly in the heterologous expression system.

We thus cloned, sequenced, and expressed the *T. aquaticus* gene encoding citrate synthase, and the recombinant enzyme was judged to have folded correctly from its similar kinetic, oligomeric, and thermostability properties compared with the native enzyme. One feature of particular note is the relationship between thermoactivity and thermostability of the enzyme. That is, the T_{opt} for activity (assayed over a period of 1 min) was found to be 80°C, yet the enzyme at the even higher temperature of 85°C had a half-life of 70 min, as measured by irreversible thermal inactivation. Clearly, it is not the enzyme's thermo*stability* that is limiting its thermo*activity*. A general model describing such a phenomenon has been recently suggested by Daniel et al. (2001), where it is proposed that an active enzyme is in equilibrium with an inactive form, and it is the inactive

form that undergoes irreversible thermal inactivation. Thus the T_{opt} for activity is determined by the temperature-induced shift in equilibrium from active to inactive forms, giving a genuine temperature optimum that is lower than the temperature at which irreversible denaturation takes place. This is indeed the case for the *Thermus* citrate synthase, which has a T_m value of 101°C as determined by DSC. Furthermore, this melting temperature is between that of the enzymes from *P. furiosus* and those of *T. acidophilum* and *S. solfataricus*; it is thus an interesting protein to model structurally and to compare possible mechanisms of thermostabilization with respect to the three archaeal citrate synthases already studied.

The homology model of the *Thermus* enzyme, and in particular the spatial conservation of putative substrate binding and catalytic amino acids, indicate an homologous enzyme that has the same basic catalytic mechanism as proposed for eukaryotic (e.g., Kurz et al. 1998; Gu et al. 1999), archaeal (Kurz et al. 2000) and Gram-negative (Nguyen et al. 2001) citrate synthases. It was then of interest to compare structural features proposed to contribute to the thermostability of the archaeal citrate synthases with the equivalent structures in the *T. aquaticus* enzyme. Most notable was the nature of the subunit interactions, where we propose that the *T. aquaticus* dimer has an ionic network interconnecting residues of the interfacial helices G and M (Fig. 3). As described in the Results section, this is almost identical in conformation to that found in the *P. furiosus* citrate synthase, four amino acids being identical and the fifth (Glu 109) possibly substituting for the archaeal Asp113. The participation of Asp113 in the ionic network of the *Pyrococcus* enzyme is made possible by the presence of *cis*-Pro115 in the loop containing the aspartate residue (Fig. 3). This normally less-favored conformation of proline induces a distinct kink in the loop, thereby enabling Asp113 to make strong ionic bonds with three other residues within the network (Russell et al. 1997). There is no equivalent proline residue in this loop region of the *T. aquaticus* citrate synthase, but the longer side chain of Glu109 in a more compact loop may still enable some of the ionic interactions to take place.

In the less stable citrate synthases from *T. acidophilum* and *S. solfataricus*, the nature of the inter-subunit interactions at helices G and M are predominantly hydrophobic, although the *T. acidophilum* enzyme has a single ionic bond in this region and the *S. solfataricus* protein has two (not networked). The mesophilic pig enzyme interface has no ionic bonds between helices G and M, and the interface is of a lower hydrophobicity than in the two archaeal enzymes. Therefore, it appears that the bacterial enzyme fits precisely into the trends observed for the archaeal citrate synthases, namely that there is an increase in ionic interactions with increasing thermostability, and that ionic networks are found in the hyperthermophilic range.

The presence of an almost identical ionic network in the bacterial and archaeal citrate synthases argues that the hyperthermostability of this enzyme was 'solved' before the divergence of their two evolutionary lineages. To the best of our knowledge, this is one of the clearest examples of bacterial and archaeal proteins using the same stabilizing ionic network mechanism, although the phenomenon has also been reported in, for example, glutamate dehydrogenase (Yip et al. 1998; Knapp et al. 1997), triose-phosphate isomerase (Maes et al. 1999) and glyceraldehyde-3-phosphate dehydrogenase (Pappenberger et al. 1997). Finally, the most extensive inter-subunit ionic network (in terms of the number of subunits involved) exists in the 60-polypeptide enzyme, lumazine synthase, from the hyperthermophilic bacterium, *Aquifex aeolicus* (Zhang et al. 2001), but at present an archaeal homolog has not yet been studied.

Acknowledgements We are grateful to the Biotechnology and Biological Research Council, UK, for generous financial support in the form of a Research Grant to M.J.D., D.W.H and Professor G.L. Taylor (University of St Andrews, UK). E.N.K. gratefully acknowledges the European Commission for the award of a Marie Curie Individual Fellowship to visit the University of Bath and also thanks the Knut and Alice Wallenberg Foundation for their financial support. Finally, we are grateful to Mrs Janice Young, AstraZeneca, Macclesfield, UK, for the N-terminal sequencing of the protein.

References

Arnott MA, Michael RA, Thompson CR, Hough DW, Danson MJ (2000) Thermostability and thermoactivity of citrate synthases from the thermophilic and hyperthermophilic Archaea, *Thermoplasma acidophilum* and *Pyrococcus furiosus*. J Mol Biol 304:657–668

Bell GS (1999) Crystallographic studies of central metabolic enzymes from the hyperthermophilic Archaea *Pyrococcus woesei* and *Sulfolobus solfataricus*. PhD thesis, University of Bath, UK

Bradford MM (1974) A rapid and sensitive method for the quantitation of microgram quantities of protein utilising the principle of protein-dye binding. Anal Biochem 72:248–254

Collaborative Computational Project (1994) Project number 4. The CCP4 suite: programs for protein crystallography. Acta Cryst D50:760–763

Connaris H, West SM, Hough DW, Danson MJ (1998) Cloning and over-expression in *Escherichia coli* of the gene encoding citrate synthase from the hyperthermophilic archaeon *Sulfolobus solfataricus*. Extremophiles 2:61–66

Daniel RM, Danson MJ, Eisenthal R (2001) The temperature optima of enzymes: a new perspective on an old phenomenon. Trends Biochem 26:223–225

Danson MJ, Hough DW (1998) Structure, function and stability of enzymes from the Archaea. Trends Microbiol 6:307–314

Eisenthal R, Cornish-Bowden A (1974) The direct linear plot. A new graphical procedure for estimating enzyme kinetic parameters. Biochem J 139:715–720

Gerike U, Hough DW, Russell NJ, Dyall-Smith ML, Danson MJ (1998) Citrate synthase and 2-methylcitrate synthase: structural, functional and evolutionary relationships. Microbiol 144:929–935

Gu Z, Drueckhammer DG, Kurz L, Liu K, Martin DP, McDermott A (1999) Solid state NMR studies of hydrogen bonding in a citrate synthase inhibitor complex. Biochemistry 38:8022–8031

James KD, Russell RJM, Parker L, Daniel RM, Hough DW, Danson MJ (1994) Citrate synthases from the Archaea: development of a biospecific affinity chromatography purification procedure. FEMS Microbiol Lett 119:181–186

Jones TA, Zhou JY, Cowan SW, Kjeldgaard M (1991) Improved methods for building protein models in electron density maps and the location of errors in these models. Acta Cryst A47:110–119

Karshikoff A, Ladenstein R (2001) Ion pairs and the thermotolerance of proteins from hyperthermophiles: a 'traffic rule' for hot roads. Trends Biochem 26:550–556

Knapp S, de Vos WM, Rice D, Ladenstein R (1997) Crystal structure of glutamate dehydrogenase from the hyperthermophilic Eubacterium *Thermotoga maritima* at 3.0Å resolution. J Mol Biol 267:916–932

Kurz LC, Nakra T, Stein R, Plungkhen W, Riley M, Hsu F, Drysdale GR (1998) Effects of changes in three catalytic residues on the relative stabilities of some of the intermediates and transition states in the citrate synthase reaction. Biochemistry 37:9724–9737

Kurz LC, Drysdale G, Riley M, Tomar MA, Chen J, Russell RJM, Danson MJ (2000) Kinetics and catalytic mechanism of citrate synthase from the thermophilic Archaeon *Thermoplasma acidophilum*. Biochemistry 39:2283–2296

Laemmli U (1970) Cleavage of the structural proteins during assembly of the head of bacteriophage T4. Nature 227:680–685

Luthy R, Bowie JU, Eisenberg D (1992) Assessment of protein models with three-dimensional profiles. Nature 356:83–85

Maes D, Zeelen JP, Thanki N, Beauchamp N, Alvarez M, Thi MH, Backmann J, Martial JA, Wyns L, Jaenicke R, Wierenga RK (1999) The crystal structure of triose-phosphate isomerase (TIM) from *Thermotoga maritima* : a comparative thermostability structural analysis of ten different TIM structures. Proteins 15:441–453

Muir JM, Russell RJM, Hough DW, Danson MJ (1995) Citrate synthase from the hyperthermophilic archaeon *Pyrococcus furiosus*. Prot Eng 8:583–592

Nguyen NT, Maurus R, Stokell DJ, Ayed A, Duckworth HW, Brayer GD (2001) Comparative analysis of folding and substrate binding sites between regulated hexameric type II citrate synthases and unregulated type I enzymes. Biochemistry 40:13177–13187

Pappenberger G, Schurig H, Jaenicke R (1997) Disruption of an ionic network leads to accelerated thermal denaturation of D-glyceraldehyde-3-phosphate dehydrogenase from the hyperthermophilic bacterium *Thermotoga maritima*. J Mol Biol 274:676–683

Plotnikov VV, Brandts JM, Lin L-N, Brandts JF (1997) A new ultrasensitive scanning calorimeter. Anal Biochem 250:237–244

Remington S, Wiegand G, Huber R (1982) Crystallographic refinement and atomic models of two different forms of citrate synthase at 2.7 and 1.7 Å resolution. J Mol Biol 158:111–152

Russell RJM, Hough DW, Danson MJ, Taylor GL (1994) The crystal structure of citrate synthase from the thermophilic archaeon *Thermoplasma acidophilum*. Structure 2:1157–1167

Russell RJM, Ferguson JMC, Hough DW, Danson MJ, Taylor GL (1997) The crystal structure of citrate synthase from the hyperthermophilic archaeon *Pyrococcus furiosus* at 1.9 Å resolution. Biochemistry 36:9983–9994

Russell RJM, Gerike U, Hough DW, Danson MJ, Taylor GL (1998) Structural adaptations of the cold-active citrate synthase from an Antarctic bacterium. Structure 6:351–361

Sambrook J, Fritsch EF, Maniatis T (1989) Molecular cloning: a laboratory manual, 2nd edn. Cold Spring Harbor Laboratory, Cold Spring Harbor, NY

Sanger F, Nicklen S, Coulson AR (1977) DNA sequencing with chain termination inhibitors. Proc Natl Acad Sci USA 74:5463–5467

Srere PA, Brazil H, Gonen L (1963) The citrate condensing enzyme of pigeon breast muscle and moth flight muscle. Acta Chem Scand 17:S129-S134

Sterner R, Liebl W (2001) Thermophilic adaptation of proteins. Crit Rev Biochem Mol Biol 36:39–106

Sutherland KJ, Henneke CM, Towner P, Hough DW, Danson MJ (1990) Citrate synthase from the thermophilic archaebacterium *Thermoplasma acidophilum*: cloning and sequencing of the gene. Eur J Biochem 194:839–844

Sutherland KJ, Danson MJ, Hough DW, Towner P (1991) Expression and purification of a plasmid-encoded *Thermoplasma acidophilum* citrate synthase from *E coli*. FEBS Lett 282:132–134

Thompson MJ, Eisenberg D (1999) Transproteomic evidence of a loop-deletion mechanism for enhancing protein thermostability. J Mol Biol 290:595–604

Vielle C, Zeikus GJ (2001) Hyperthermophilic enzymes: sources, uses, and molecular mechanisms of thermostability. Microbiol Mol Biol Rev 65:1–43

Weitzman PDJ (1978) Anomalous citrate synthase from *Thermus aquaticus*. J Gen Microbiol 106:383–386

White O, Eisen JA, Heidelberg JF, Hickey EK, Peterson JD, Dodson RJ, Haft DH, Gwinn ML, Nelson WC, Richardson DL, Moffat KS, Qin H, Jiang L, Pamphile W, Crosby M, Shen M, Vamathevan JJ, Lam P, McDonald L, Utterback T, Zalewski C, Makarova KS, Aravind L, Daly MJ, Minton KW, Fleischmann RD, Ketchum KA, Nelson KE, Salzberg S, Smith HO, Venter JC, Fraser CM (1999) Genome sequence of the radioresistant bacterium *Deinococcus radiodurans* R1. Science 286:1571–1577

Williams R, Sharp R (1995) The taxonomy and identification of *Thermus*. In: Sharp R, Williams R (eds) *Thermus* species. Plenum, New York, pp 1–91

Yip KSP, Britton KL, Stillman TJ, Lebbink J, de Vos WM, Robb FT, Vetriani C, Maeder D, Rice DW (1998) Insights into the molecular basis of the thermal stability from the analysis of ion-pair networks in the glutamate dehydrogenase family. Eur J Biochem 255:336–346

Zhang XF, Meining W, Fischer M, Bacher A, Ladenstein R (2001) X-ray structure analysis and cristallographic refinement of lumazine synthase from the hyperthermophile *Aquifex aeolicus* at 1.6 angstrom resolution: determinants of thermostability revealed from structural comparisons. J Mol Biol 306:1099–1114